Available online at www.sciencedirect.com
ScienceDirect
Ceramics International 34 (2008) 2099–2105
CERAMICS INTERNATIONAL
www.elsevier.com/locate/ceramint

Influence of particle properties on the viscosity of polymer–alumina composites

T. Hanemann [a,b,*]

[a] Research Center Karlsruhe, Institute for Materials Research, P.O. Box 3640, D-76021 Karlsruhe, Germany
[b] Albert-Ludwigs-University Freiburg, Department of Microsystem Engineering, Georges-Köhler-Allee 102, D-79110 Freiburg, Germany

Received 9 July 2007; received in revised form 25 July 2007; accepted 13 August 2007
Available online 22 September 2007

Abstract

The influence of different micro- and nanosized alumina fillers, dispersed in an unsaturated polyester resin as polymer matrix, on the resulting composite flow behaviour was investigated systematically. It was found that the composite viscosity depends strongly on the properties of the applied particles like particle size, particle size distribution, solid load and especially on the specific surface area. The change of the relative viscosity with load can be described by using the different established semiempirical approaches for the estimation of the critical filler load. The value of the latter one decreases with increasing fillers surface area value significantly. The impact of the solid load as well as the fillers specific surface area on composite's flow behaviour will be discussed in the following.

Keywords: A. Suspensions; B. Composites; Alumina; Rheology

1. Introduction

Due to their outstanding thermomechanical properties structural ceramic materials are of a certain interest in microsystem technologies. In addition, electroceramics like PZT a.o. can be applied as actuators [1,2]. In the past various replication techniques have been established for the realization of microstructured ceramic parts. For a low cost replication the different variants of powder injection molding can be used [3–9]. The solid load of the used composite or feedstock has to be as large as possible in order to obtain a reduced shrinkage during sintering and an improved structural accuracy. Unfortunately, an increasing solid load causes a significant viscosity rise before reaching the critical filler load [8,9], which has a strong impact on the mold filling as well as on demolding, e.g. due to reduced greenbody stability. Composite reaction molding using polymer based reactive resins instead of thermoplastics or wax as fluidic binder components enables a rapid prototyping of ceramic or metal parts [10].

The change of the viscosity with solid load (volume content Φ) was first described by Einstein (1) for diluted solutions or dispersions introducing a coefficient k_E, which is 2.5 for hard particle spheres [11]. The relative viscosity η_{rel} is defined as the quotient of the apparent viscosity of the composite (η_{comp}) and the pure binder (η_{binder}). In the last 50 years a large number of different model descriptions have been developed for a correlation of the composite's relative viscosity with filler load. Considering replication via molding techniques followed by debinding and sintering the estimation of the critical filler load Φ_{max} in organic binder systems is of particular interest [8]. Quite often the approaches developed by Krieger–Dougherty (2), Quemada (3), Eilers (4), Mooney (5), Chong (6) or by Zhang and Evans (7) among others are used [12–17]. The latter one simplifies the Chong approach by substituting the factor 0.25 by a free parameter C, which allows a more flexible approximation tested successfully with a polypropylene–alumina feedstock developed for ceramic injection molding [17].

A liquids viscosity as a function of temperature can be described using an Arrhenius-type approach (Andrade equation) (8), η_1 and η_2 are the apparent viscosities at the two different temperatures T_1 and T_2, R the gas constant and ΔE_a is the flow activation energy, which depends mainly on the composition of the investigated system. Typical thermoplastic

* Correspondence to: Albert-Ludwigs-University Freiburg, Department of Microsystem Engineering, Georges-Köhler-Allee 102, D-79110 Freiburg, Germany. Tel.: +49 7247 82 2585; fax: +49 7247 82 2905.
E-mail address: thomas.hanemann@imf.fzk.de.

0272-8842/$34.00
doi:10.1016/j.ceramint.2007.08.007

binders consisting of polyethylene with stearic acid as additive show values around 32 kJ/mol [8], the addition of fillers or binder components change significantly the activation energy value.

$$\text{Einstein}: \eta_{rel} = \frac{\eta_{comp}}{\eta_{binder}} = 1 + k_E \Phi \quad (1)$$

$$\text{Krieger–Dougherty}: \eta_{rel} = \left(1 - \frac{\Phi}{\Phi_{max}}\right)^{-k_E \Phi_{max}} \quad (2)$$

$$\text{Quemada}: \eta_{rel} = \left(1 - \frac{\Phi}{\Phi_{max}}\right)^{-2} \quad (3)$$

$$\text{Eilers}: \eta_{rel} = \left(1 + \frac{1.25\Phi\Phi_{max}}{\Phi_{max} - \Phi}\right)^{2} \quad (4)$$

$$\text{Mooney}: \eta_{rel} = \exp\left(\frac{2.5\Phi\Phi_{max}}{\Phi_{max} - \Phi}\right) \quad (5)$$

$$\text{Chong}: \eta_{rel} = \left(\frac{\Phi_{max} - 0.25\Phi}{\Phi_{max} - \Phi}\right)^{2} \quad (6)$$

$$\text{Zhang and Evans}: \eta_{rel} = \left(\frac{\Phi_{max} - C\Phi}{\Phi_{max} - \Phi}\right)^{2} \quad \text{with } C \text{ as free constant} \quad (7)$$

$$\text{Arrhenius description}: \ln\frac{\eta_1(T_1)}{\eta_2(T_2)} = \frac{\Delta E_a}{R}\left(\frac{1}{T_1} - \frac{1}{T_2}\right) \quad (8)$$

In addition to feedstock development for the realization of dense ceramic parts polymer–ceramic filler composites have a strong potential for applications, e.g. in microelectronics due to the adjustable coefficient of expansion, enhanced thermal stability and improved thermo-mechanical properties [18]. The knowledge about the composite flow behaviour is essential for device fabrication or for packaging purposes also.

2. Experimental

A commercially available low viscous mixture of an unsaturated polyester resin with a polymer content around 65 wt% and styrene as reactive thinner (Roth GmbH) was used as polymer binder. All alumina fillers were dried at 250 °C for 12 h prior to dispersion in the resin. Table 1 lists all relevant particle properties like specific surface area and particle size distribution. The mixtures were processed using a laboratory dissolver stirrer (IKA Eurostar power control-visc) for 30 min at 1000 rpm under ambient conditions; trapped air was removed via ultrasonic energy. All viscosity measurements were performed at three different temperatures (20, 40, 60 °C) in the shear rate range between 1 and 100 s^{-1} using a cone and plate rheometer (CVO50, Bohlin). The experimental uncertainty of the obtained data is in the range of ±5%.

Table 1
Specifications of the used micro- and nanosized alumina

Type	Vendor	Specific surface area (m^2/g)	Measured particle sizes (μm)		
			d_{10}	d_{50}	d_{90}
CT3000SG	Almatis	6–8[a]	0.071	0.266	1.002
RCHP	Baikowski	7–9[a]	0.242 (d_{20})	0.335	0.575
TM DAR	Taimei	12.8	0.104	0.165	0.297
Nanotek	Nanophase	34	0.125	0.155	0.192
C	Degussa	107	0.125	0.155	0.205

[a] Vendor's data.

3. Results and discussion

3.1. Flow behaviour

The influence of CT3000SG on the viscosity of unsaturated polyester resins have been described earlier [19,20]. The particle properties of RCHP, especially the specific surface area, are similar to the ones of CT3000SG (Table 1), therefore a comparable behaviour can be expected. Fig. 1 shows in the shear rate between 1 and 100 s^{-1} and at three different temperatures the viscosity of two different unsaturated polyester–RCHP composites.

At a low load of 3.1 vol% (10 wt%) a Newtonian flow behaviour at 20 and 60 °C occurs. The flow anomaly at 40° and in the shear rate range between 2 and 10 s^{-1} has been observed earlier and is typical for the used polyester resin [19]. At a large load of 40.3 vol% (70 wt%) the flow curve is more complex: at 20 °C the viscosity increases with shear rate followed by a descent. At 40 °C and larger shear rates dilatant flow behaviour can be observed; only at 60 °C an almost Newtonian flow can be measured. As expected at large loads the viscosity values are significantly larger than the related ones at lower alumina contents.

In contrast to CT3000SG and RCHP the TM DAR alumina possesses a larger specific surface area and a smaller average particle size around 165 nm. At all investigated temperatures the viscosity curves are noisier than in the RCHP-based systems (Fig. 2). Especially at the large TM DAR content of 40.3 vol% the viscosities at 40 and 60 °C are larger than in the related

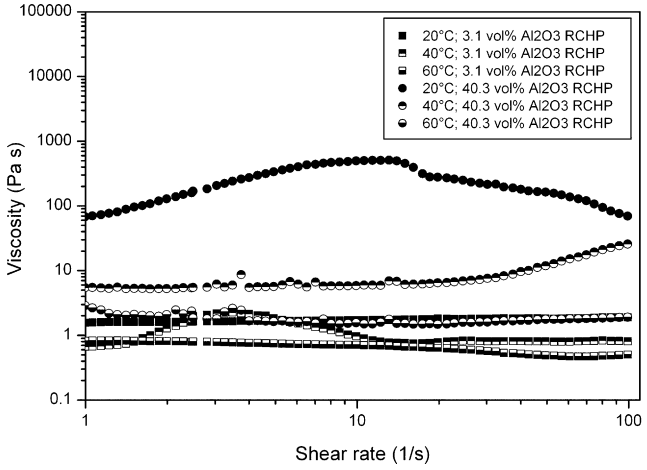

Fig. 1. Composite viscosity at low and high RCHP load at three different temperatures in the shear rate range between 1 and 100 s^{-1}.

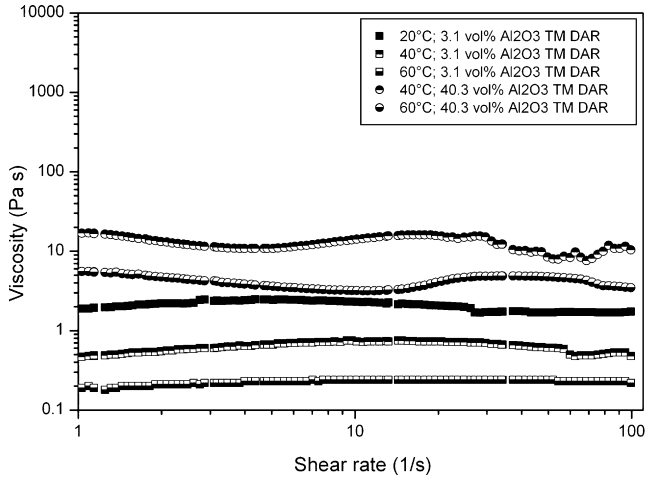

Fig. 2. Composite viscosity at low and high TM DAR load at three different temperatures in the shear rate range between 1 and 100 s^{-1}.

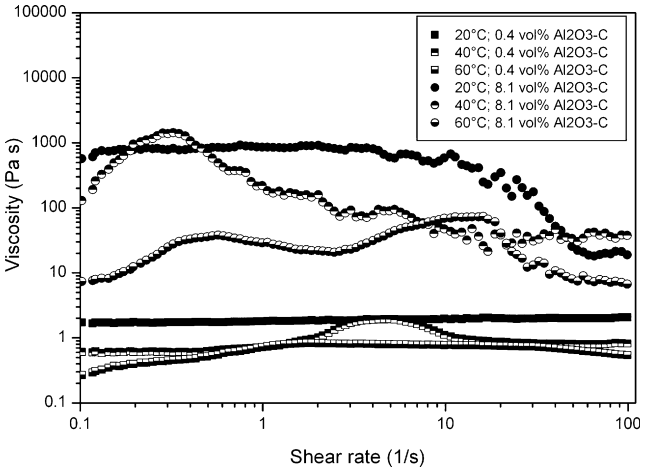

Fig. 4. Composite viscosity at low and high Al_2O_3–C load at three different temperatures in the shear rate range between 1 and 100 s^{-1}.

RCHP filled resins; at 20 °C it was not possible to measure a viscosity curve.

The Nanotek filler shows a similar particle size distribution as the TM DAR alumina, but the specific surface area is with a value around 34 m^2/g significantly increased. Even at a low load of 1.6 vol% (5 wt%) viscosity values which are similar to the ones of 3.1 vol% TM DAR in the polyester resin can be found. Increasing loads change the flow curve from an almost Newtonian to a pronounced pseudoplastic type, larger loads than 23.4 vol% cannot be realized (Fig. 3).

An unequivocal influence of the fillers surface area on the resulting composite flow behaviour can be seen in Fig. 4. The largest accessible load is around 8.1 vol% (20 wt%), the viscosities at lower shear rates and at 20 and 40 °C are very large; the flow curves are noisy and a pseudoplastic flow occurs. At 60 °C and large shear rates the viscosity values are larger than the values for the lower measuring temperatures. That unusual viscosity–temperature behaviour can be an indicator for an overfeed composite system. Hence, this mixture with a load of 8.1 vol% is omitted for the estimation of the critical filler load and flow activation energy in the following sections.

3.2. Estimation of the critical filler load

3.2.1. Alumina with small specific surface areas

The application of the different empirical models (2)–(7) for the description of the relative viscosity (1) with filler load allows the estimation of the critical filler load considering constant experimental parameters like binder composition, temperature and shear rate. Fig. 5 shows the relative viscosity of all investigated composites using the unsaturated polyester resin as binder and the different alumina with increasing solid load at 60 °C and a shear rate of 100 s^{-1}. Whereas the viscosities for the different CT3000SG and RCHP containing composites are almost similar, increasing values can be found for the TM DAR based mixtures. The use of CT3000SG, RCHP and TM DAR allows a load around 40 vol%. The addition of alumina with larger specific surface area and larger amounts of smaller particles reduces the accessible maximum filler load significantly, only a solid content around 23.4 vol% can be achieved using the Nanotek alumina (34 m^2/g specific surface area). In case of the alumina C only a small load of 8.1 vol% is possible, which can be explained with the large specific surface

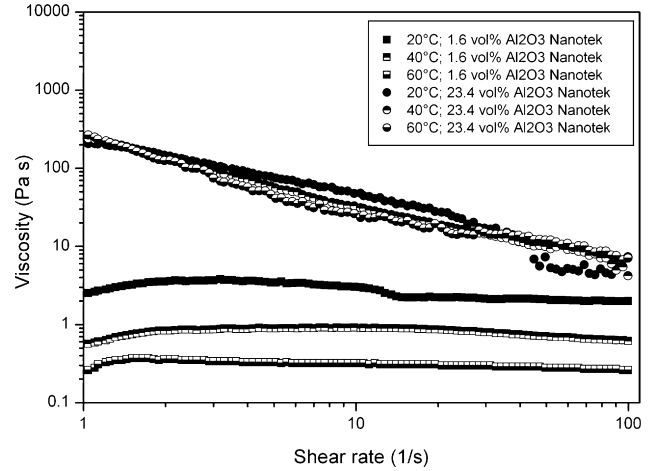

Fig. 3. Composite viscosity at low and high Nanotek load at three different temperatures in the shear rate range between 1 and 100 s^{-1}.

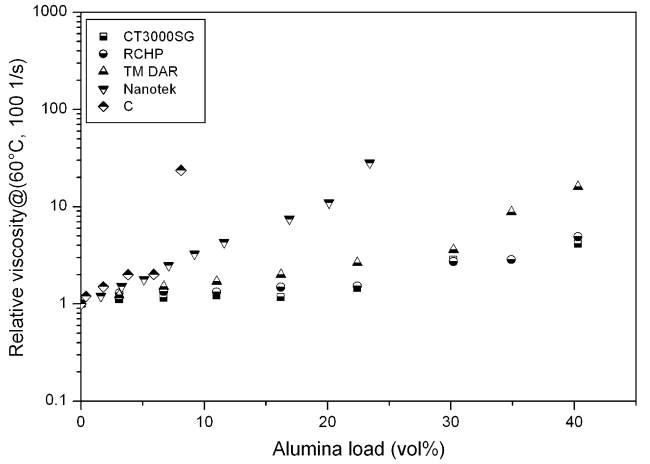

Fig. 5. Relative viscosity change with alumina load at 60 °C and a shear rate of 100 s^{-1}.

Table 2
Estimated critical filler load and stability index at different temperatures applying different empirical models describing the relative viscosity of polyester–CT3000SG composites

	Critical filler load Φ_{max} (and related fit stability index R^2)		
	20 °C	40 °C	60 °C
Krieger–Dougherty	0.41 (0.74)	0.47 (0.96)	0.78 (0.95)
Quemada	0.47 (0.90)	0.59 (0.99)	0.80 (0.95)
Chong	0.46 (0.86)	0.54 (0.98)	0.69 (0.96)
Eilers	0.44 (0.81)	0.52 (0.97)	0.79 (0.95)
Mooney	0.55 (0.84)	0.71 (0 97)	–[a]
Zhang–Evans	0.57 (0.97)	0.64 (1.00)	0.65 (0.96)

[a] Unreasonable calculated Φ_{max} value of 1.4.

Table 4
Estimated critical filler load and stability index at different temperatures applying different empirical models describing the relative viscosity of polyester–TM DAR composites

	Critical filler load Φ_{max} (and related fit stability index R^2)		
	20 °C	40 °C	60 °C
Krieger–Dougherty	0.43 (0.87)	0.43 (0.92)	0.44 (0.95)
Quemada	0.58 (0.96)	0.51 (0.90)	0.54 (0.98)
Chong	0.52 (0.93)	0.48 (0.98)	0.50 (0.98)
Eilers	0.49 (0.90)	0.47 (0.96)	0.48 (0.97)
Mooney	0.67 (0.90)	0.60 (0.97)	0.63 (0.98)
Zhang–Evans	–[a]	0.52 (0.99)	0.52 (0.99)

[a] Unreasonable calculated Φ_{max} value of 1.1.

area of 107 m^2/g. A similar behaviour was observed earlier using unsaturated polyester resin filled with micro- and nanosized silica [21].

Table 2 lists for the polyester resin–CT3000SG composite the estimated critical filler load Φ_{max} and the related fit stability index R^2 at all investigated temperatures using the different empirical models (2)–(7). Preliminary results concentrating only on one temperature (20 °C) have been published earlier and agree with the data presented in this section [19]. At 20 °C only the Quemada and the Zhang–Evans models deliver fit results with acceptable stability index R^2, the suggested values for the critical filler load between 0.47 and 0.57 seems to be realistic, the Chong and Mooney approaches yield similar values. At higher temperatures the fit quality is in all cases significantly improved, only the Mooney model shows at 60 °C an unreasonable value for the critical filler load of 1.4. With increasing temperatures all models suggest larger critical filler loads, at 40 °C between values between 0.47 and 0.71 and at 60 °C between 0.69 and 0.78. Following the values for the fit stability index the Zhang–Evans model delivers the best critical filler load at all investigated temperatures, the obtained Φ_{max} values seem to be realistic. Composites containing the RCHP–alumina can be described with almost all used empirical models (Table 3), only at 60 °C the Mooney-model delivers once again unreasonable values for 60 °C as in the CT3000SG filled systems. The values for the fit stability index R^2 are better than 0.94, the calculated critical filler loads are realistic under the given experimental conditions.

Table 3
Estimated critical filler load and stability index at different temperatures applying different empirical models describing the relative viscosity of polyester–RCHP composites

	Critical filler load Φ_{max} (and related fit stability index R^2)		
	20 °C	40 °C	60 °C
Krieger–Dougherty	0.42 (0.97)	0.42 (0.99)	0.47 (0.95)
Quemada	0.48 (1.00)	0.49 (0.90)	0.49 (0.99)
Chong	0.46 (1.00)	0.47 (0.94)	0.49 (1.00)
Eilers	0.45 (0.99)	0.45 (0.97)	0.45 (0.99)
Mooney	0.56 (1.00)	0.56 (0.96)	–[a]
Zhang–Evans	0.47 (1.00)	0.42 (1.00)	0.47 (1.00)

[a] Unreasonable calculated Φ_{max} value of 1.2.

The application of the different empirical models on the polyester–TM DAR composites yields acceptable results, especially at the lowest measurement temperature the quality of the approximation, following the values of the fit stability index, is reduced (Table 4). Considering all investigated temperatures the Quemada, Chong and Mooney models yield the best results, the Zhang–Evans description can only be used at 40 and 60 °C but there with an excellent quality. Exemplarily the Quemada, Mooney and Zhang–Evans approximations are shown in Fig. 6. The suitability of these models has been successfully proved in the description of filled wax or polymer melts [22–24].

For better comparison Table 5 lists the average critical filler loads calculated by using all investigated empirical models for the microsized alumina. For an improved reliability only the estimations with a fit stability index better than 0.90 have been considered. Following the particle properties given in Table 1, CT3000SG should allow the largest critical filler load, followed by RCHP and TM DAR. Besides the specific surface area the particle size distribution shows some impact on the accessible load. Multimodal mixtures of spherical particles, which contain particle fractions with a size difference by a factor of 6.5, allow

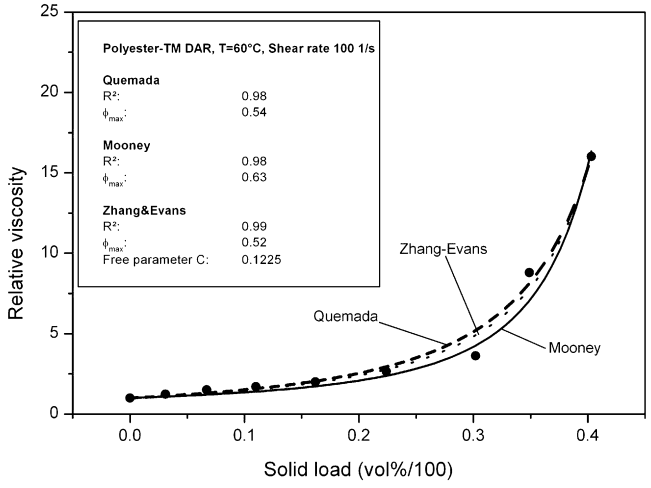

Fig. 6. Empirical description of relative viscosity change with TM DAR load using the Quemada, Money and Zhang–Evans approaches (T = 60 °C, shear rate = 100 s^{-1}).

Table 5
Comparison of the calculated average critical filler loads

	Calculated average critical filler load Φ_{max}		
	20 °C	40 °C	60 °C
CT3000SG	0.52	0.58	0.74
RCHP	0.47	0.47	0.47
TM DAR	0.57	0.50	0.52

the realization of solid loads larger than 74% (dense sphere packing). At the lower measuring temperatures the calculated average critical loads show a non-uniform behaviour, at 60 °C CT3000SG a large average critical filler load around 0.74 has been estimated. In contrast to RCHP and TM DAR, CT3000SG possesses a broad particle size distribution between 0.1 and 1.0 μm, enabling, to some extent, a multimodal arrangement, hence a large solid load beyond the value for a random dense sphere packing of 64% should be reasonable.

3.2.2. Alumina with large specific surface areas

A semiempirical or phenomenological description of the relative viscosity change with nanoparticle load is hardly to be found in literature, previous work investigated the influence of nanosized silica (Aerosil®) on the flow behaviour of an unsaturated polyester resin [21]. Table 6 lists for the composite system polyester resin–Nanotek alumina the estimated critical filler load and the related fit stability index using the different model descriptions mentioned. Following the values for the fit quality the approximations are worse in comparison to the ones for the microsized alumina, especially at the lower measuring temperatures no useful fit can be obtained. Only at the highest temperature of 60 °C the Quemada and the Zhang–Evans and, with some limitations, the Chong approaches deliver realistic values for the critical filler load around 30 vol%. In contrast the change of the relative viscosity with solid alumina C load can be quite reliably described using the Krieger–Dougherty, Quemada, Eilers, and especially at all temperatures, the Zhang–Evans approaches. Critical filler loads between 8 and 10 vol% have been calculated, which seems to be reasonable (Table 7).

Table 6
Estimated critical filler load and stability index at different temperatures applying different empirical models describing the relative viscosity of polyester–Nanotek composites

	Critical filler load Φ_{max} (and related fit stability index R^2)		
	20 °C	40 °C	60 °C
Krieger–Dougherty	0.25 (0.12)	0.24 (0.10)	0.23 (0.83)
Quemada	0.39 (0.68)	0.36 (0.66)	0.29 (0.99)
Chong	0.35 (0.58)	0.33 (0.58)	0.27 (0.97)
Eilers	0.29 (0.25)	0.28 (0.24)	–[a]
Mooney	0.35 (0.27)	0.33 (0.25)	0.28 (0.90)
Zhang–Evans	–[a]	–[a]	0.30 (0.99)

[a] Calculation of unreasonable values.

Table 7
Estimated critical filler load and stability index at different temperatures applying different empirical models describing the relative viscosity of polyester–alumina C composites

	Critical filler load Φ_{max} (and related fit stability index R^2)		
	20 °C	40 °C	60 °C
Krieger–Dougherty	0.08 (0.43)	0.08 (0.95)	0.08 (1.00)
Quemada	0.10 (0.75)	0.09 (0.99)	0.10 (0.97)
Chong	0.10 (0.69)	0.09 (1.00)	0.07 (0.08)
Eilers	0.08 (0.45)	0.08 (0.99)	0.08 (1.00)
Mooney	0.35 (0.27)	0.33 (0.25)	0.28 (0.90)
Zhang–Evans	0.77 (0.98)	0.08 (1.00)	0.09 (1.00)

3.3. Estimation of the flow activation energy

The influence of temperature on the composite's viscosity can be described using an Arrhenius type Eq. (8) within a small temperature interval calculating the flow activation energy ΔE_a. Large ΔE_a values correspond with a pronounced sensitivity of the viscosity to temperature changes [8]. The numerical value depends on the inner polymer chain friction, the free volume, the intermolecular interaction between the polymer chains and the dispersed filler particles. Typical values for pure waxes, which can be treated as low molecular mass oligomers with only small molecular entanglement, are in the range between 4.4 kJ/mol (paraffine, short aliphatic chains) and 19 kJ/mol (polyethylene wax, long aliphatic chains). Molten thermoplastic polymers with a pronounced polymer chain entanglement show larger values up to 32 kJ/mol (polypropylene) [8]. Exemplarily Fig. 7 shows for the different polyester–alumina C composites the typical Arrhenius diagram with an increase of the logarithmic viscosity with load in the temperature range between 20 and 60 °C. Table 8 lists the corresponding flow activation energy ΔE_a and the related fit stability index R^2 for the different alumina C load in polyester. With increasing solid load a pronounced increase of the flow activation energy can be observed, which can be explained with the increasing interaction of the nanosized particles with the polymer. Due

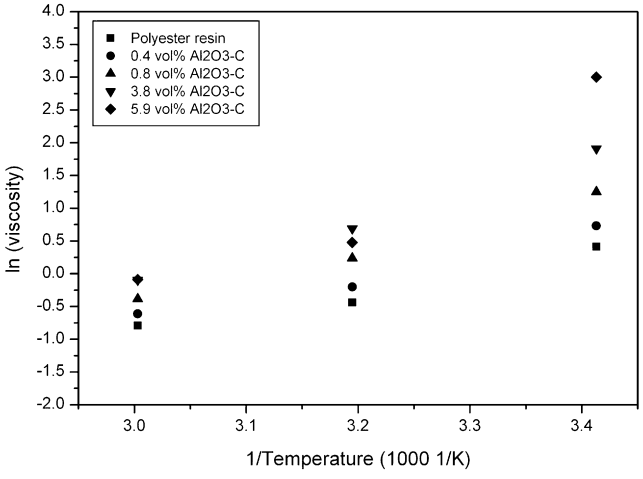

Fig. 7. Arrhenius diagram of polyester–alumina C composites.

Table 8
Estimation of the flow activation energy ΔE_a for polyester–alumina C composites

	Flow activation energy (kJ/mol)	Fit stability index R^2
Pure polyester resin	8.2	0.96
0.4 vol% alumina C	9.1	0.97
0.8 vol% alumina C	11.1	0.99
3.8 vol% alumina C	13.8	0.99
5.9 vol% alumina C	21.1	0.90

to the large surface area a huge binder volume is attached to the particles surface reducing the polymer's mobility. Hence, an improved inner friction occurs, which can be overcome only at higher temperatures.

For a better comparison Fig. 8 shows for all investigated alumina the relative flow activation energy change $\Delta\Delta E_a$ with load referred to the pure polyester resin. With exception of the Nanotek alumina increasing alumina loads cause an increase of the flow activation energy; this is in agreement with literature [8]. A significant impact of the solid content on the flow activation energy can only be observed at concentrations where a pronounced viscosity increase can be detected (Fig. 5). A clear interpretation of the flow activation energy is difficult. Two opposite effects superimpose with increasing filler load. On the one hand, due to the decrease of the polymer volume fraction, the influence of polymer entangling processes is reduced; hence the temperature influence should be lowered too. On the other hand, due to a significant mismatch in the individual thermal coefficients of expansion between the polymer and the filler, which causes at constant weight fraction a change in the volume fraction of each compound with temperature, an increase of the flow activation energy with load should be expected [8].

Previous investigations examined the influence of surfactants attached to the CT3000SG surface on the viscosity, critical filler load and flow activation energy [19,20]. A surface treatment of the hydrophilic alumina with different polyethylene glycol surfactants converts the fillers surface polarity from hydrophilic to hydrophobic. An unequivocal correlation between surfactant chemical structure, HLB-value (hydrophilic–lipophilic balance), concentration, composite viscosity and flow activation energy cannot be observed [19]. In a rough and cautious approximation dispersants like Brij72 (small HLB-value around 5), which cause a composite viscosity reduction, lower the flow activation energy slightly with increasing concentration. The opposite behaviour, that means an increase of the composite viscosity as well as flow activation energy with increasing dispersant concentration, can be observed in case of Brij98 (large HLB-value around 15) [20].

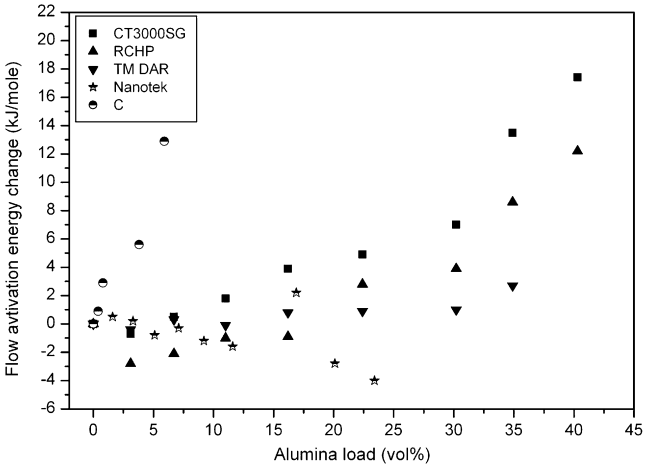

Fig. 8. Flow activation energy change with load relative to the pure polyester.

A comparable behaviour was described by Attarian et al. [25]. The addition of ethylene–vinyl acetate (EVA) to aluminium silicate–polyethylene wax composites reduced the flow activation energy from 14.6 down to 6.8 kJ/mol at constant solid load and shear rate. One comprehensible explanation can be the more polar character of EVA in comparison to the used wax, which enables a better wetting of the inorganic filler like a dispersant increasing the compatibility of the polar filler and the non-polar main binder component. In a different system a clear correlation between filler content (56–67%) and flow activation energy for porcelain–PE-based binder composites could not be observed either [22]. Quite recently the influence of a silane coupling agent treatment of an aluminium particle with a alumina surface in a bisphenol-A type epoxy resin was described. A pronounced viscosity reduction was found [26].

4. Conclusions

The flow behaviour of a polymer based reactive resin, filled with different micro- and nanosized alumina, was characterized intensely. Besides the solid load particle properties, especially the specific surface area, have a pronounced impact on the composite's viscosity. Using microsized alumina with a specific surface area of 10 m^2/g or less dispersions with 40 vol% load can be realized easily. Increasing surface area values reduce the accessible solid load down to 8 vol% (specific surface area around 107 m^2/g). In almost all investigated systems and measuring temperatures the critical filler load can be estimated by the different established semiempirical models. Especially the Zhang–Evans model, proved at ceramic feedstock systems, is suitable for composites filled with micro- as well as nanosized alumina. Increasing solid load or increasing surface area values cause a pronounced elevation of the composite's flow activation energy.

Acknowledgements

TH thanks the Deutsche Forschungsgemeinschaft (DFG) for financial support within the framework of the Sonderforschungsbereich SFB 499 as well as the European Commission for the funding within the 4M-Network of Excellence.

References

[1] J. Hausselt, H.-J. Ritzhaupt-Kleissl, R. Ruprecht, Ceramics in microtechnology—materials, processing, design, in: IMAPS/ACerS Proceedings First International Conference and Exhibition on Ceramic Interconnect

and Ceramic Microsystems Technologies (CICMT), Baltimore, USA, April 10–13, (2005), pp. 211–221.
[2] A.J. Moulson, J.M. Herbert, Electroceramics, John Wiley & Sons Ltd., Chichester, UK, 2003, pp. 339–409.
[3] W. Bauer, R. Knitter, G. Bartelt, A. Emde, D. Göhring, E. Hansjosten, Replication techniques for ceramic microcomponents with high aspect ratios, Microsyst. Technol. 9 (2002) 81–86.
[4] V. Piotter, N. Holstein, K. Plewa, R. Ruprecht, J. Hausselt, Replication of micro components by different variants of injection molding, Microsyst. Technol. 10 (2004) 547–551.
[5] S. Rath, L. Merz, K. Plewa, P. Holzer, T. Gietzelt, J. Hausselt, Isolated metal and ceramic micro parts in the sub-millimeter range made by PIM, Adv. Eng. Mater. 7 (2005) 619–622.
[6] L. Liu, N.H. Loh, B.Y. Tay, S.B. Tor, Y. Maurakoshi, R. Maeda, Mixing and characterisation of 316L stainless steel for micro powder injection molding, Mater. Charact. 54 (2005) 230–238.
[7] R. Zauner, Micro powder injection molding, Microelectron. Eng. 83 (2006) 1442–1444.
[8] R.G. German, Powder Injection Molding, Metal Powder Industries Federation, Princeton, 1990.
[9] R. Tandon, Metal injection molding, in: Encyclopedia of Materials: Science and Technology, Elsevier Science Ltd., Oxford, 2001, pp. 5439–5442.
[10] T. Hanemann, K. Honnef, J. Hausselt, Process chain development for the rapid prototyping of microstructured polymer, ceramic and metal parts: composite flow behaviour optimization, replication via reaction molding and thermal postprocessing, Int. J. Adv. Manuf. Technol. 33 (2007) 167–175.
[11] A. Einstein, Eine neue Bestimmung der Moleküldimension, Ann. Physik. 19 (1906) 289–306;
A. Einstein, Berichtigung zu meiner Arbeit: Eine neue Bestimmung der Moleküldimension, Ann. Physik. 34 (1911) 591–592.
[12] I.M. Krieger, T.J. Dougherty, A mechanism for non-newtonian flow in suspensions of rigid spheres, Trans. Soc. Rheol. III (1959) 137–152.
[13] D. Quemada, Rheology of concentrated disperse systems and minimum energy dissipation principle. I. Viscosity–concentration relationship, Rheol. Acta 16 (1977) 82–94.
[14] J.S. Chong, E.B. Christiansen, A.D. Baer, Rheology of concentrated suspensions, J. Appl. Polym. Sci. 15 (1971) 2007–2021.
[15] M. Mooney, The viscosity of a concentrated suspension of spherical particles, J. Colloid Sci. 6 (1951) 162–170.
[16] H. Eilers, Die Viskosität von Emulsionen hochviskoser Stoffe als Funktion der Konzentration, Kolloid-Zeitschrift 97 (1941) 313–321.
[17] T. Zhang, J.R.G. Evans, Predicting the viscosity of ceramic injection moulding suspensions, J. Eur. Ceram. Soc. 5 (1989) 165–172.
[18] R.K. Goyal, A.N. Tiwari, U.P. Mulik, Y.S. Negi, Novel high performance Al_2O_3/poly(ether ether ketone) nanocomposites for electronic applications, Compos. Sci. Technol. 67 (2007) 1802–1812.
[19] T. Hanemann, Influence of dispersants on the flow behaviour of unsaturated polyester–alumina-composites, Compos. A: Appl. Sci. Manuf. 37 (2006) 735–741.
[20] T. Hanemann, Viscosity change of unsaturated polyester–alumina-composites using polyethylene glycol alkyl ether based dispersants, Compos. A: Appl. Sci. Manuf. 37 (2006) 2155–2163.
[21] T. Hanemann, R. Heldele, J. Hausselt, Particle size dependent viscosity of polymer–silica-composites, in: Proceedings 4M 2006—Second International Conference on Multi-Material-Micro-Manufacture (4M), Grenoble, France, September 20–22, (2006), pp. 191–194.
[22] I. Agote, A. Odriozola, M. Gutierrez, A. Santamaria, J. Quintanilla, P. Coupelle, J. Soares, Rheological study of waste porcelain feedstocks for injection molding, J. Eur. Ceram. Soc. 21 (2001) 2843–2853.
[23] T. Kitano, T. Kataoka, T. Shirota, An empirical equation of the relative viscosity of polymer melts filled with various inorganic fillers, Rheol. Acta 20 (1981) 207–209.
[24] J.J. Reddy, N. Ravi, M. Vijayakumar, A simple model for viscosity of powder injection molding mixes with binder content above powder critical binder volume concentration, J. Eur. Ceram. Soc 20 (2000) 2183–2190.
[25] M. Attarian, E. Taheri-Nassaj, P. Davami, Effect of ethylene-vinyl acetate copolymer on the rheological behaviour of alumino-silicate/polyethylene wax suspensions, Ceram. Int. 28 (2002) 507–514.
[26] J. Xu, C.P. Wong, Characterization and properties of an organic–inorganic dielectric nanocomposite for embedded decoupling capacitor applications, Compos. A: Appl. Sci. Manuf. 38 (2007) 13–19.